Direct Measurement of Actin Polymerization Rate Constants by Electron Microscopy of Actin Filaments Nucleated by Isolated Microvillus Cores

THOMAS D. POLLARD and MARK S. MOOSEKER
Department of Cell Biology and Anatomy, Johns Hopkins University School of Medicine, Baltimore, Maryland 21205, and Department of Biology, Yale University, New Haven, Connecticut 06520

ABSTRACT We used actin filament bundles isolated from intestinal brush-border microvilli to nucleate the polymerization of pure muscle actin monomers into filaments. Growth rates were determined by electron microscopy by measuring the change in the length of the filaments as a function of time. The linear dependence of the growth rates on the actin monomer concentration provided the rate constants for monomer association and dissociation at the two ends of the growing filament. The rapidly growing ("barbed") end has higher association and dissociation rate constants than the slowly growing ("pointed") end. The values of these rate constants differ in 20 mM KCl compared with 75 mM KCl, 5 mM $MgSO_4$. 2 μM cytochalasin B blocks growth entirely at the barbed end, apparently by reducing both association and dissociation rate constants to near zero, but inhibits growth at the pointed end to only a small extent.

It is well established that the formation of protein polymers such as bacterial flagella, actin filaments, and microtubules involves at least two steps: nucleation and elongation (17). In the case of actin there is also a breaking-annealing step. We will focus on the elongation process, which involves the addition of a monomer (c_1) to extend a polymer (c_n) by one unit:

$$c_1 + c_n \underset{k_-}{\overset{k_+}{\rightleftharpoons}} c_{n+1}.$$

This process can be described by the equation:

$$\frac{dl}{dt} = k_+ (c_1) - k_-,$$

as shown for bacterial flagella (2) where l is the length. The polymer grows longer when $k_+ (c_1) > k_-$. An apparent equilibrium is achieved when $k_+ (c_1) = k_-$, and the apparent equilibrium constant is:

$$K_{app} = \frac{k_+}{k_-} = \frac{1}{c_1^0}.$$

This steady-state monomer concentration, c_1^0, has been called the critical concentration for polymerization (17), because every increment of subunit concentration above this critical concentration results in an equal increment of polymer formation.

This formulation is successful when the growth of the polymer is unidirectional as in the case of bacterial flagella or when the polymer is not polar (as, for example, in the hypothetical case of a double helical polymer with antiparallel chains such as DNA). However, this formulation is likely to be inadequate when the polymer is polarized the way that actin (9) and microtubules (6) are, making subunit addition vectorial and nonequivalent at the two ends. Direct evidence for nonequivalent subunit addition at the two ends of actin filaments (22, 7, 11) and microtubules (5, 1) came from electron microscopy showing different rates of net growth at the two ends of morphologically identifiable nuclei. In the case of actin the two ends were identified by decoration with myosin "arrowheads." The "barbed" (B) end is fast; the "pointed" (P) end is slow. In the case of microtubules the two ends were identified relative to the polarity of cilia or flagella. The basal end is slow, the distal end is fast.

The realization that the reactions at the two ends are unique opened the possibility that the equilibria at the two ends are different, with the consequence that there might be a steady-state flux of molecules through the polymer (21). This steady-state flux has also been called "head-to-tail" polymerization (21) or "treadmilling" (14). Steady-state flux occurs when the c_1^0 differs at the two ends, making dl/dt positive at one end and negative at the other. For actin, the steady-state monomer concentration is that where $dl^B/dt = -dl^P/dt$.

Evidence for a steady-state flux in actin filaments came from the time-course of the equilibration of labeled actin monomers

THE JOURNAL OF CELL BIOLOGY · VOLUME 88 MARCH 1981 654-659

with fully polymerized actin (21). Treadmilling in microtubules was first suggested by the kinetics of labeled monomer incorporation into a steady-state sample of microtubules (14). Another way to evaluate the steady-state flux is to measure the reaction rate constants at the two ends directly as Bergen and Borisy (3) have done for microtubules.

An analysis of the elongation mechanism of actin requires the evaluation of each reaction which may lead to the addition or loss of a monomer. For actin, eight reactions have been considered (Fig. 1).[1] In addition to the reactions shown here, there is, at some unknown point, the hydrolysis of the bound ATP, because ultimately all of the actin molecules in the filament have a bound ADP (17). In experiments where excess ATP is present in the medium, the addition of monomer with bound ADP is disregarded. Usually, the loss of a monomer with bound ATP is also dismissed (17, 21), but there is no justification for this.[2] Consequently, elongation of actin can be described by two equations:

$$\frac{dl^{B}}{dt} = k_{+}^{B,T}(c_1) - k_{-}^{B}$$

$$\frac{dl^{P}}{dt} = k_{+}^{P,T}(c_1) - k_{-}^{P},$$

where $k_{-}^{B} = k_{-}^{B,T} + k_{-}^{B,D}$ and $k_{-}^{P} = k_{-}^{P,T} + k_{-}^{P,D}$.

As pointed out previously (17, 3), these equations have the form of $y = mx + b$, so that plot of dl/dt vs. (c_1) should be linear with k_+ given by the slope and the k_- given by the y intercept. This is true for the elongation of both bacterial flagella (17) and microtubules (3).

The present work is an analysis of the rate constants for actin polymerization. These rate constants were obtained by using electron microscopy to measure the rate of actin filament growth at the ends of morphologically identifiable nuclei, bundles of actin filaments isolated from intestinal microvilli. These microvillus cores have three advantages over the heavy meromyosin-decorated actin filaments used as nuclei in earlier studies: (*a*) they are more stable; (*b*) they can be used in ATP; and (*c*) up to 10 actin filaments can grow from each end. The rate constants obtained by electron microscopy have provided considerable insight into the mechanism of actin polymerization and the approach has allowed us to define more quantitatively than previously possible the mechanism by which the fungal product cytochalasin B inhibits actin polymerization.

MATERIALS AND METHODS

Purified monomeric actin was prepared from rabbit skeletal muscle (13) by extraction from an acetone powder, a cycle of polymerization and depolymerization, and gel filtration on a 2.5 × 50 cm or a 1.5 × 40 cm column of Sephadex G-150 medium (equilibrated with buffer G consisting of 2 mM Tris-Cl, 0.5 mM dithiothreitol, 0.2 mM ATP, 0.2 mM $CaCl_2$) to remove actin oligomers and minor contaminating proteins.

Chicken intestinal epithelial cell brush borders were isolated according to Mooseker et al. (16). Microvilli were released from these brush borders by homogenization and separated from the brush border remnants by differential centrifugation (8). These microvilli were suspended in MV buffer (75 mM KCl, 5 mM Mg SO_4, 0.1 mM dithiothreitol, 0.1 mM phenylmethylsulfonyl fluoride, 10 mM imidazole-Cl, pH 7.5) containing 1% Triton X-100 to remove the membranes. The microvillus cores were collected by centrifugation at 18,000 rpm in a Beckman JA-20 rotor (Beckman Instruments, Inc., Spinco Div., Palo Alto, Calif.) for 10 min at 4°C and washed once in MV buffer or polymerization buffer consisting of 20 mM KCl, 0.1 mM $MgSO_4$, 1 mM EGTA, 0.1 mM phenylmethylsulfonyl fluoride, 10 mM imidazole-Cl, pH 7.0 and used within 6 h.

Chicken breast muscle myosin subfragment-1 was prepared by Dr. Daniel Kiehart by chymotryptic digestion (19) and purified by chromatography on Sephacryl S-200 in 0.5 M KCl, 10 mM EDTA, 10 mM imidazole-Cl, pH 7.0, 0.02% sodium azide.

Electron microscope polymerization experiments were carried out at 22°C in MV buffer or polymerization buffer, with a fixed concentration of microvillus cores (~0.05 mg protein/ml) and various concentrations of monomeric actin between 1.2 and 7.2 μM. The final mixture contained 0.2 part of G buffer. Samples were incubated from 5 to 200 s for control and 20 s to 20 min for samples with 2 μM cytochalasin B, depending on the growth rates. These conditions were selected such that growth rates were constant and that the actin monomer concentration did not fall more than ~1% during the time sampled. The reactions were terminated by very gentle dilution with 4 vol of buffer, and diluted samples were immediately applied to Formvar- and carbon-coated, glow-discharged hydrophilic grids, using care to avoid filament breakage. After 10-15 s, the bulk of the sample drop was removed by touching a filter paper to the edge of the grid and replaced by a drop of 1% aqueous uranyl acetate for 15 s. After removal of the bulk of the stain with filter paper, the grid was allowed to air dry. To establish that this sample preparation method did not alter the length of the actin filaments, we compared the effect of diluting samples fourfold into polymerization buffer with or without 50 mM glutaraldehyde for 0, 60, or 120 s. In this case, the sample was made with nuclei of subfragment-1-decorated actin filaments and 5 μM actin polymerized for 20 s in 20 mM KCl. We found no change in the length of new actin filaments during 120 s at the critical concentration either with or without glutaraldehyde. This is ~10 times longer than required for us to dilute our samples for rate measurements. The grids were examined in JEOL 100-CX or Philips 201 electron microscopes. We photographed microvillus cores that had neither end obscured by residual membrane, which exhibited actin filament growth from at least one end, and which were not obviously damaged during specimen preparation. The polarity of the actin filaments was established in parallel samples decorated with myosin subfragment-1 (15). For decoration of the filaments, grids were washed with two drops of polymerization buffer, reacted with a drop of a 100 μg/ml subfragment-1 for 1 min, and then stained.

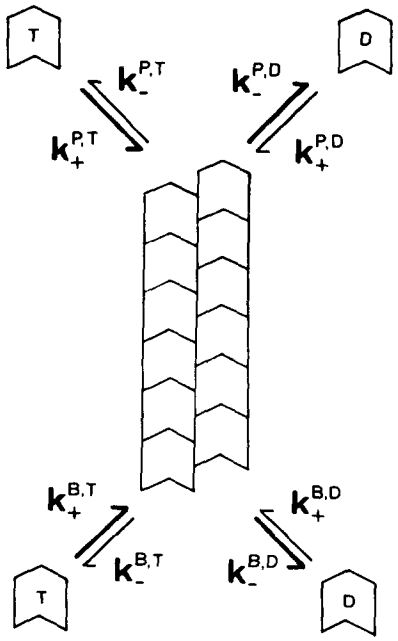

FIGURE 1 A model of actin polymerization. The symbols are defined in the text. The generally accepted pathways of association and dissociation are indicated by heavier arrows. The polarity of the subunits in the double helical actin filament, is indicated by a chevron shape.

[1] We suggest that a slight modfication of Oosawa and Asakura's nomenclature be used for the rate constants. Subscript + or − will be used to denote on or off steps; superscript B or P will be used to denote barbed or pointed end; and superscript T or D will be used to denote bound ATP or ADP. If any of the on or off reactions is found to have multiple steps, these can be denoted k_{+1}, k_{+2}, etc.

[2] It has been argued by Woodrum et al. (22) that because the subunit addition process is vectorial, nucleotide hydrolysis may also be vectorial, resulting in there being ATP bound to the terminal subunit (or subunits) at one of two ends. At that end, at least, the dissociation of a monomer with bound ATP would be expected.

The length of nucleated actin filaments was measured with a map reader or digitizer. The number measured for each time point varied from 10 to 50, but most samples consisted of ~25 filaments. Growth rates were calculated from the mean lengths at specific time points. Slopes and intercepts of the dependence of these growth rates on monomer concentration were calculated by least squares linear regression.

Viscometric polymerization experiments were carried out at 25°C in 20 mM KCl, 10 mM imidazole, pH 7, with 0.25 part buffer G plus 0.7 μM, polymerized actin nuclei, and several concentrations of gel-filtered actin monomer. Polymerization was measured with Ostwald capillary viscometers (size 150, Cannon Instrument Co., State College, Pa.) with buffer flow times of ~30 s. The initial rate of elongation was taken as the change in $(\eta)^{1/1.8}$ with time to account for the fact that the viscosity of a solution containing a constant number of filaments is approximately proportional to $(\text{length})^{1.8}$ (18). At the highest actin concentrations (14 μM) the initial rates were measured during the first 1-2 min. At low actin concentrations the initial rate of the viscosity changes was constant for >2 min.

Materials were obtained from the following sources: Tris base, dithiothreitol, ATP, Sephadex G-150-120, imidazole, Triton X-100, EGTA, and cytochalasin B from Sigma Chemical Co. (St. Louis, Mo.); bovine pancreatic alpha-chymotrypsin, Worthington Biochemical Corp. (Freehold, N. J.); phenylmethylsulfonyl fluoride from Eastman Organic Chemicals Div., Eastman Kodak Co. (Rochester, N. Y.); Sephacryl S-200 from Pharmacia Fine Chemicals, Div. Pharmacia Inc. (Piscataway, N. J.)

RESULTS

The quantitative analysis of the actin filament elongation mechanism requires measurement of elongation rates at the two ends of the filament. As we describe in detail in another manuscript (Mooseker and Pollard, manuscript in preparation), actin polymerization can be nucleated by the bundle of actin filaments isolated from the intestinal microvillus (Fig. 2). The filaments grow more rapidly from one end than the other. The fast end has been identified as the "barbed" end by myosin subfragment-1 decoration. The slow end is the "pointed" end. The net rate of growth in the two directions was measured by sampling the reaction of actin monomer with microvillus bundles at several time points (Fig. 3). The filaments grow at constant rates from both ends. At 7 μM monomer (Fig. 3), the rate at the fast "barbed" end is six times the rate at the slow "pointed" end. Because of the large difference in growth rates at the two ends, it was difficult to collect reliable data for growth rates at the slow end, because the filaments remain short during the period of linear growth, particularly at low monomer concentration.

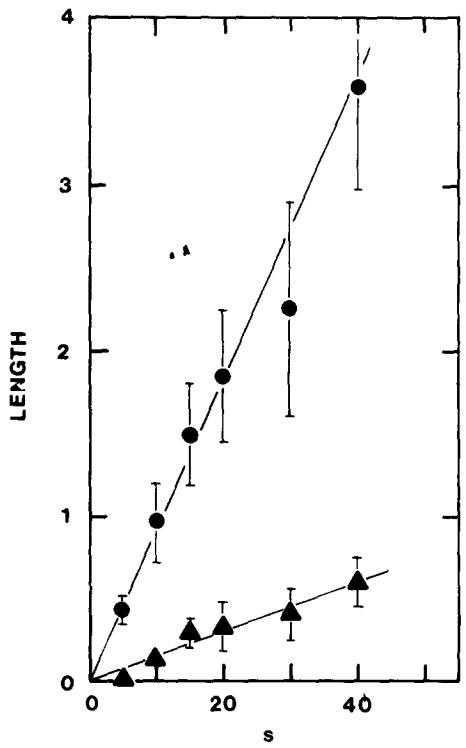

FIGURE 3 Time-course of the growth of actin filaments from the barbed (●) and pointed (▲) ends of microvillus cores in 20 mM KCl buffer with 7.2 μM actin monomer. Mean length (± 1 SD) in micrometers is plotted vs. time in seconds.

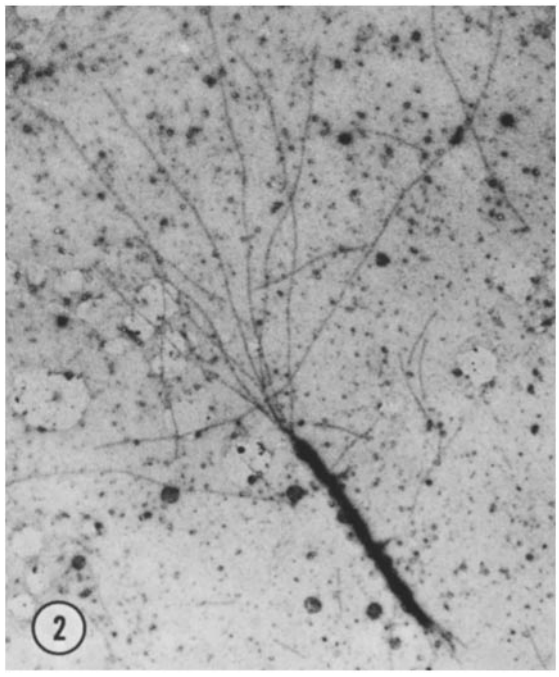

FIGURE 2 An electron micrograph of a negatively stained microvillus core used to nucleate polymerization of 5.7 μM actin for 20 s. Longer filaments have grown from the upper barbed end than the pointed end. × 13,100.

Plots of filament growth rates against monomer concentration can be fitted well with straight lines (Fig. 4). Each plot intersects the x axis (where this growth rate is zero) at the critical concentration for that end. Note that in 20 mM KCl (Fig. 4 b) and in 75 mM KCl, 5 mM $MgSO_4$ (Fig. 4 *a*) and at all monomer concentrations the barbed end grows faster than the pointed end. In 20 mM KCl, the x intercepts for the barbed and pointed ends are the same, at least within experimental error. In 75 mM KCl, 5 mM $MgSO_4$ the x intercepts for the two ends are apparently different. The two conditions tested were selected because they represent extremes. On one hand, in KCl/$MgSO_4$ the rate and extent of actin polymerization are maximal. On the other hand, 20 mM is close to the lowest concentration of KCl where actin polymerization is complete and rate of polymerization is very low (see for example reference 12).

The data in Figs. 3 and 4 are consistent with the model of actin polymerization presented in the Introduction. The rate constants derived from these plots are summarized in Table I. The k_+'s are the slopes and the k_-'s are the y intercepts of the plots in Fig. 4. Similar results were obtained in one additional KCl/Mg and two additional 20 mM KCl experiments.

In 2 μM cytochalasin B, the growth rate at the pointed end is normal in KCl/Mg and reduced by ~60% in 20 mM KCl, but no growth was observed at the barbed end in either buffer (Fig. 4). The absence of growth at the barbed end could have

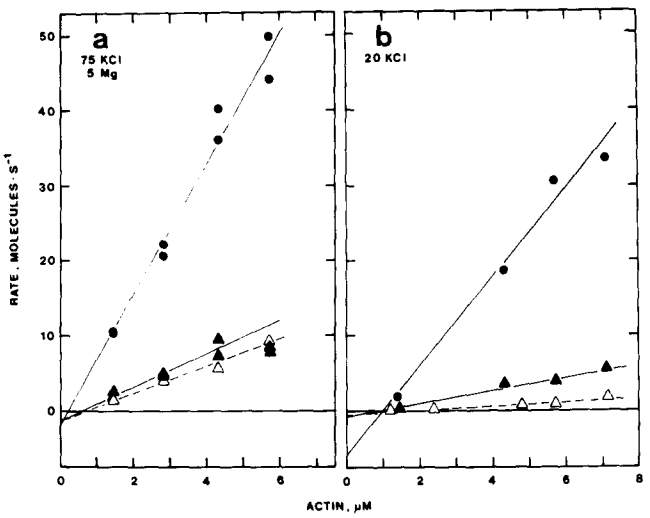

FIGURE 4 Dependence of actin filament growth rates on actin monomer concentration in either the 75 mM KCl, 5 mM $MgSO_4$ buffer (left) or the 20 mM KCl buffer (right). ●, barbed end; ▲, pointed end control; △, pointed end with 2 μM cytochalasin B. No growth was observed at the barbed end in cytochalasin B. In the KCl/Mg experiment, growth rates at two time points for each actin concentration are plotted. In the 20-mM KCl experiment, mean growth rates measured from three or more time points are plotted. Correlation coefficients were >0.98 except for the control pointed end in KCl/Mg (▲) (0.96 omitting the 5.6 μM actin data as shown; 0.90 including all of the data) and the pointed end in 20 mM KCl with cytochalasin B (△) (0.86).

TABLE I

20 mM KCl	$k_+^{B,T}$	$k_+^{P,T}$	k_-^B	k_-^P
Control	5.9	0.8	6.0	0.7
CB	~0	0.3	~0	0.6
75 mM KCl 5 mM $MgSO_4$				
Control	8.8	2.2	2.0	1.4
CB	~0	1.8	~0	1.3

Units: k_+, molecules·s^{-1}·μM^{-1}; k_-, s^{-1}.

been caused by a reduction in the rate of monomer association or an increase in the rate of monomer dissociation or both, but the absence of growth at any monomer concentration up to 7.2 μM made it impossible to evaluate events at the barbed end from electron microscopy alone.

A viscometric experiment (Fig. 5) ruled out an increase in the rate of monomer dissociation at the barbed end in cytochalasin B. In this experiment the rate of actin filament elongation was estimated as the rate of change of the 1.8th root of the viscosity under conditions where the number of filaments was constant. The constancy of filament number during the initial 10-20% of the viscosity change was assured by using conditions (20 mM KCl) where nucleation is negligible during the time of interest (12) and by adding a constant amount of polymerized actin as nuclei. In both the presence and absence of 2 μM cytochalasin B, the initial growth rates were linear functions of the monomer concentration (Fig. 5 *a*) and the critical concentrations were the same (Fig. 5 *b*). Because the *y* intercept of the cytochalasin B data is less than the *y* intercept of the control data, the absence of growth at the barbed end in cytochalasin B in the electron microscopy experiment (Fig. 4 *b*) cannot be caused by an increase in the monomer dissociation rate at the barbed end.

Because the critical concentration for polymerization is the same at both ends in 20 mM KCl and because cytochalasin B does not affect the critical concentration at the pointed end, the overall critical concentration for polymerization in 20 mM KCl is the same in the presence or absence of cytochalasin B (Fig. 5 *b*). In contrast, in 75 mM KCl, 5 mM $MgSO_4$ cytochalasin B raises the overall critical concentration by ~1.2 μM in

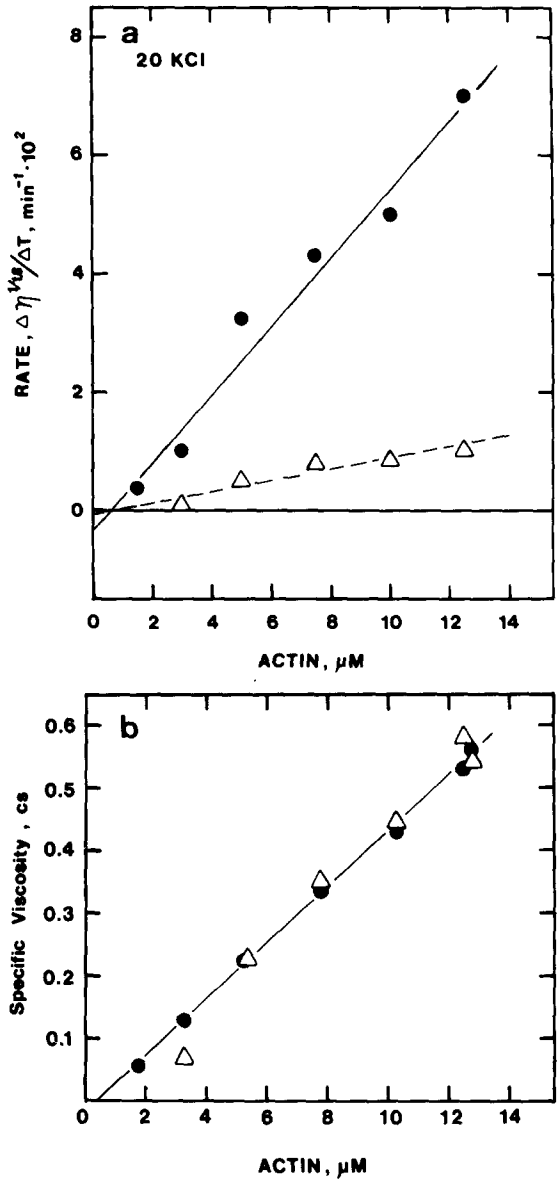

FIGURE 5 Viscometric analysis of the actin concentration dependence of the rate and extent of actin polymerization in 20 mM KCl as described in Materials and Methods. ●, control; △, 2 μM cytochalasin B. The initial rates of elongation from actin filament nuclei were measured as the rate of change of the 1.8th root of the specific viscosity. The extent of polymerization was measured on the samples after a 4-h incubation. In fitting the steady-state viscosity data by linear regression, the viscosity with 3.2 μM actin in cytochalasin B was omitted, because this sample had clearly not reached steady state in 4 h. The *x* intercepts of the two rate plots were made equal, because the steady-state viscosities extrapolated to the same critical concentration.

viscometric experiments (not shown), because the critical concentration at the pointed end is higher than that at the barbed end (Fig. 4).

DISCUSSION

This is the first attempt to measure the rate constants for polymerization at the two ends of the actin filament. The method is the same applied successfully by Bergen and Borisy (3) to analyze microtubular growth. The great advantages of this method are that events at the two ends of the polymer are assessed independently and that rates can be measured in absolute terms. The disadvantages are that it is tedious, that some error may be introduced by artifactual breakage of the filaments during the specimen preparation, and that the polymers may not all start growing simultaneously because of the presence of naturally occurring inhibitors of subunit addition at the end(s) of the actin filaments of the isolated microvillus cores. These and other unrecognized factors must all contribute to the large standard deviations in the length measurements. Moreover, these factors probably lead to a minimal estimate for the growth rates. Nevertheless, the plots of growth rate vs. subunit concentration are remarkably linear with typical correlation coefficients >0.98 for the fast end. At the slow end the data are not as good, largely because the filaments grow so slowly compared to the fast end. To avoid subunit depletion because of growth at the barbed end, samples must be taken when the growth at the slow end is minimal. Nonetheless, even the pointed end data fit linear plots reasonably well.

As in the case of microtubules, the end favored for subunit association is also the end favored for subunit dissociation. This is seen more clearly in 20 mM KCl. Nevertheless, during polymerization in the presence of subunit concentrations $> c_l^{o,P}$ there is net growth at both ends and the efficiency is reasonably high. For example, when $c_l = 10\ c_l^o$ the efficiency is ~90%: that is, during the time it takes to add 10 subunits at either end, only one subunit dissociates. The plots also explain why polymerization is faster in KCl/Mg than in 20 mM KCl. This is caused in part by slightly greater k_+'s, but is principally caused by smaller k_-'s, especially at the barbed end.

Because k_+^B is close to that of diffusion-limited processes and k_+^P is considerably less, it is possible that elongation at the pointed end is tightly linked to and limited by a slower reaction that follows the formation of the collison intermediate. The dephosphorylation of the bound ATP is one possible such reaction. It may follow then that monomer addition at the barbed end is not coupled to ATP hydrolysis. This would account for the lag observed for ATP hydrolysis compared with polymerization (4).

The rate constants for actin association and dissociation are generally similar to those determined for tubulin association to and dissociation from the ends of microtubules (3). The actin association rate constants we measured are considerably larger (~10 molecules · s^{-1} · μM^{-1}) than those estimated previously by a combination of light-scattering and electron microscopy (~10^{-2} molecules · s^{-1} · μM^{-1}) by Wegner (20) in 1 mM $CaCl_2$. We have not examined polymerization in 1 mM $CaCl_2$, so that it is possible that the difference is attributable to the difference in the experimental conditions.

The rate constants can be used to predict steady-state subunit flux ("treadmilling") rates. In 20 mM KCl, the critical concentrations are the same at the two ends so that there is no subunit flux. In KCl/Mg the critical concentrations are different at the two ends, so at steady state there can be net addition at the barbed end balanced by net loss at the pointed end. From the rate constants in Table I the flux rate is estimated to be 0.7 molecules · s^{-1} and Wegner's (21) "s" value (the "head-to-tail" parameter) is 0.2. This means that, at steady state, one of every five cycles of subunit association and dissociation contributes to the flux. Note, however, that the flux rate is considerably lower than the elongation rates under the conditions usually employed in laboratory experiments (10–25 μM actin monomer).

The experiments also demonstrate conclusively that the major effect of CB is on the barbed end. This confirms the qualitative analysis of MacLean-Fletcher and Pollard (12). There is also a small effect of CB on growth of the pointed end, especially in 20 mM KCl, which was not recognized previously. By use of the viscometric experiment to put limits on the unobserved events at the barbed end, it appears that CB inhibits growth at the barbed end by reducing both the association and dissociation rate constants to nearly zero. Thus CB actually blocks the barbed end.

The electron microscope experiments demonstrate that the simple viscometric analysis of the actin polymerization process can be extremely misleading. One example is the strikingly different results obtained by viscometry and by electron microscopy of nucleated actin polymerization in cytochalasin B in buffers where the rate of polymerization is fast. In previous studies (12) it was found that 2 μM cytochalasin B inhibited the rate of the viscosity change by <20% in KCl/Mg, while in reality (Fig. 4*a*) elongation at the barbed end is blocked altogether and the overall rate of elongation is reduced by >80%. This discrepancy is likely to be related to the fact that the assembly of actin filaments from actin monomers is a complex process involving three overlapping but separate reactions. Isolating a single discrete step such as elongation is difficult with an averaging technique like viscometry.

These experiments are obviously only the first steps in elucidating the detailed mechanism of actin polymerization. In future experiments efforts must be made to improve the precision of the rate measurements. This will make it possible to examine in detail the kinetic constants and critical concentrations for the two ends under a variety of conditions. One needed improvement will be some way to study the growth of the two ends independently because their widely differing growth rates have made measurements at the slow end very difficult. An analysis of pure pointed end growth may now be possible using a new "capping protein" from *Acanthamoeba* (10) which seems to nucleate actin polymerization but, like CB, blocks growth in the barbed direction.

We would like to thank Daniel Kiehart for the myosin subfragment-1, John Cooper for help with a control, Janelle Levy for carrying out some viscometry experiments, and Edwin Taylor for his comments on the interpretation of the experiments. This work was supported by National Institutes of Health research grants GM-26132 and AM-2538.

Received for publication 25 August 1980, and in revised form 11 December 1980.

REFERENCES

1. Allen, C. A., and G. G. Borisy. 1974. Structural polarity and directional growth of microtubules of *Chlamydomonas* flagella. *J. Mol. Biol.* 90:381–402.
2. Asakura, S. 1968. A kinetic study of *in vitro* polymerization of flagella. *J. Mol. Biol.* 35: 237–239.
3. Bergen, L. G., and G. G. Borisy. 1980. Head-to-tail polymerization of microtubules *in vitro*. Electron microscope analysis of seeded assembly. *J. Cell Biol.* 84:141–150.
4. Brenner, S. L., and E. D. Korn. 1980. Effects of cytochalasins on actin polymerization and actin ATPase provide insights into the mechanism of polymerization. *J. Biol. Chem.* 255: 841–844.

5. Dentler, W. L., S. Granett, G. B. Witman, and J. L. Rosenbaum. 1974. Directionality of brain microtubule assembly *in vitro*. *Proc. Natl. Acad. Sci. U.S.A.* 71:1710–1714.
6. Erickson, H. P. 1974. Microtubule surface lattice and subunit structure and observations on reassembly. *J. Cell Biol.* 60:153–167.
7. Hayashi, T., and W. Ip. 1976. Polymerization polarity of actin. *J. Mechanchem. Cell Motil.* 3:163–169.
8. Howe, C. L., M. S. Mooseker, and T. A. Graves. 1980. Brush-border calmodulin. A major component of the isolated microvillus core. *J. Cell Biol.* 85:916–923.
9. Huxley, H. E. 1963. Electron microscope studies on the structure of natural and synthetic protein filaments from striated muscle. *J. Mol. Biol.* 7:281–308.
10. Isenberg, G. H., U. Aebi, and T. D. Pollard 1980 A novel actin binding protein from *Acanthamoeba* which regulates actin filament polymerization and interactions. *Nature.* 288:455–459.
11. Kondo, H., and S. Ishiwata. 1976. Unidirectional growth of F-actin. *J. Biochem.* 79:159–171.
12. MacLean-Fletcher, S., and T. D. Pollard. 1980. Mechanism of action of cytochalasin B on actin. *Cell.* 20:329–341.
13. MacLean-Fletcher, S., and T. D. Pollard. 1980. Identification of a factor in conventional muscle actin preparation which inhibits actin filament self-association. *Biochem. Biophys. Res. Commun.* 96:18–27.
14. Margolis, R. L., and L. Wilson. 1978. Opposite end assembly and disassembly of microtubules at steady state *in vitro*. *Cell.* 13:1–8.
15. Mooseker, M., and T. Pollard. 1980. Assembly of actin onto microvillus cores and demonstration that cytochalasin B blocks the preferred assembly end. *Fed. Proc.* 39:1660.
16. Mooseker, M., T. Pollard, and K. Fujiwara. 1978. Characterization and localization of myosin in the brush border of intestinal epithelial cells. *J. Cell Biol.* 79:444–453.
17. Oosawa, F., and S. Asakura. 1975. Thermodynamics of the Polymerization of Protein. Academic Press, Inc., London.
18. Tanford, C. 1961. Transport processes: viscosity. *In* Physical Chemistry of Macromolecules. John Wiley & Sons, Inc., New York. 317–456.
19. Weeds, A. G., and R. S. Taylor. 1975. Separation of subfragment-1 isoenzymes from rabbit skeletal muscle myosin. *Nature (Lond.).* 257:54–56.
20. Wegner, A. 1975. Kinetics of the cooperative association of actin to actin filaments. *Biophys. Chem.* 3:215–225.
21. Wegner, A. 1976. Head-to-tail polymerization of actin. *J. Mol. Biol.* 108:139–150.
22. Woodrum, D. T., S. A. Rich, and T. D. Pollard. 1975. Evidence for the biased bidirectional polymerization of actin using heavy meromyosin produced by an improved method. *J. Cell Biol.* 67:231–237.